

Robust retrieval of a seismic point-source time function

S. Kravanja,¹ G. F. Panza^{1,2} and J. Šílený³

¹ Dipartimento di Scienze della Terra, Università degli Studi di Trieste, Via E. Weiss 4, 34127 Trieste, Italy

² International Centre for Theoretical Physics, SAND Group, Miramare, 34100 Trieste, Italy

³ Geophysical Institute, Acad. Sc. Czech Rep., Bocni II/1401, 14131 Praha 4, Czech Republic

Accepted 1998 September 4. Received 1998 August 17; in original form 1997 May 27

SUMMARY

A comparison of two waveform-inversion methods designed to retrieve the mechanism of a seismic source and of its time function is presented using vertical-component synthetic signals, computed for velocity with a maximum frequency of 10 Hz. The geometry of the array of recording stations simulates the northeastern Italy Seismometric Network (OGS Trieste), consisting of 16 stations of which 12 are short period, vertical component only, three are short period, three components, and one is broad band. The synthetic seismograms are inverted using an inconsistent forward modelling technique; that is, by means of Green's functions (GFs) constructed for a structural model different from those used to generate the synthetic data. The approach based on 'overparametrization' of the rupture process, by means of independent moment tensor rate functions (MTRFs), and their subsequent reduction to the source time function (STF) (Method I) is shown to be superior to a traditional approach where the rupture process is constrained *a priori* (Method II). With Method I, the effects of inconsistent structural modelling are partially absorbed into the uncorrelated parts of the MTRFs and their reverse slips, which allows us to eliminate them by subsequent retention of the STF as their positively constrained correlated part. Method I is shown to be able to yield a reasonable estimate of the STF even in the case when the traditional approach fails completely. Inadequacy of the GF, which may occur due to mislocation of the hypocentre, is taken into account by comparing the two approaches: the source depth is optimized simultaneously with the determination of the mechanism and the source time function. In addition to its capacity to handle inaccurate structural models, the overparametrization yielding a linear inverse scheme is completely independent from the starting model of the mechanism: Method II, using a gradient scheme, can proceed properly only if the starting source parameters are sufficiently close to the true ones. The extension of the comparison of the performances between the two methods to an M_d 3.0 earthquake near Friuli, in February 1988, recorded by seven stations of the OGS Trieste Network gives results in good agreement with the synthetic tests. The orientation of the nodal planes retrieved using Method I is in good agreement with the orientation of the source mechanism retrieved from the polarity of first arrivals, while Method II gives consistent results only when starting from the source parameters retrieved using Method I.

Key words: inversion, model, seismic structure, synthetic waveforms.

INTRODUCTION

Together with the retrieval of the focal mechanism of a seismic event, waveform inversion also offers the possibility of determining the source time function (STF). There are many approaches to this task, with the data to be inverted ranging from teleseismic records to local seismograms. Frequently, the inversion methods incorporate the parametrization of the source

process into the moment tensor (Stump & Johnson 1977) (or, alternatively, the double couple, if exclusively tectonic earthquakes are treated), and the STF, which appears as a product in the equation relating the source to the radiated wavefield. Because retrieval of the double couple is non-linear, the process of recovering a focal mechanism and the STF needs an iterative scheme for minimization of the misfit function comprising the residual between the observed and

synthetic seismograms. If a typical gradient method is used, a sufficiently good starting point in the model space of the source parameters must be available to guarantee convergence (e.g. Langston, Barker & Pavlin 1982; Nabelek 1984). This is frequently not the case, especially if weak events on a local scale (characterized by relatively high frequencies and a low signal-to-noise ratio) are to be treated. However, the non-linearity is not an inherent feature of the problem but it was introduced artificially. An alternative approach, which does not destroy the linearity of the moment tensor description of the source even when its rupture history is sought, was introduced by Sipkin (1982). He proposed retaining the MTRFs as independent functions of time to keep the linearity of the inverse problem. Sipkin designed this method for teleseismic data where he was interested in the mechanism only, and did not determine the STF. His approach was extended to local waveforms by Koch (1991a,b), but he did not retrieve the rupture history either. The method that allows us to retrieve the rupture history was designed by Sileny, Campus & Panza (1992), who complemented the linear inversion with a subsequent step which reduces the independent MTRFs to the moment tensor and the STF. Alternative ways of performing this reduction were suggested by Ru & Tichelaar (1990) and Vasco (1989).

If we do not follow the concept of empirical GFs (Hartzell 1978), or the approaches of clustered event processing which avoid explicit use of GFs completely (e.g. Dahm 1996), all methods assume a perfect knowledge of the parameters of the medium between the source and the points of observation, which is necessary for the construction of the GFs. However, this is the exception rather than the rule, and in reality we always have only rough estimates of the true structure. This is not a difficulty if we do not search for fine details of the rupture process; that is, if we can constrain our data set to low frequencies. In this case, the wavelength is large compared with the details of the structure which may be poorly known, and the recovered source parameters are not distorted significantly. However, if waves are to be inverted which 'see' such details in the medium, then all the features of the medium that are not resolved in the GFs are thrown into the source where they appear as spurious signals contaminating especially the STF. Thus, it is highly desirable to use an inversion method that takes into account the fact that the structural model which is available may not be appropriate. The method of Sileny, Panza & Campus (1992) (Method I) satisfies this requirement: thanks to the 'overparametrization' of the rupture process, by means of independent MTRFs and their subsequent reduction to a positive STF, it has the capacity partly to absorb in the MTRFs the artefacts introduced by the inappropriate modelling of the medium, and then to minimize them during the factorization of the MTRFs. The goal of this contribution is to demonstrate this capability in comparison with a traditional method (Method II) that applies the positivity constraint to the STF *a priori*.

THEORY

Method I proceeds basically in two steps. First, the MTRFs are determined as six independent time functions as the solution of a linear inverse problem. This is essentially the approach of Sipkin (1982), extended by introducing a damping of the normal equations to be solved (Koch 1991) and by

using a triangular parametrization of the MTRFs (Nabelek 1984). The linear inverse problem may be built into an iterative procedure in the case where we do not consider the hypocentre as a fixed point but allow it to change its depth (Silený *et al.* 1992) or to move inside a pre-defined volume (Silený & Pšencik 1995) to balance the effect of mislocation. Moreover, there is the option to consider simultaneously two structural models which may be acceptable for the area under study and to 'mix' the GFs in an optimum ratio to reach the best fit of the synthetics to the observed data. However, since we aim to demonstrate the ability of the method to provide us with a reasonable estimate of the STF even when we deal with an inexact model of the medium, this option is not taken in the following experiments.

The second step reduces the six independent MTRFs, $\dot{M}_{ij}(t)$, into the constant moment tensor M_{ij} and the STF, $\dot{M}(t)$, $\dot{M}_{ij} \rightarrow M_{ij}\dot{M}(t)$. This is a non-linear inverse problem that is solved iteratively and in which constraints are imposed on the source parameters to be determined. The 'predicted' values of the MTRFs, $M_{ij}\dot{M}(t)$, are matched to the 'observed' MTRFs; that is, to those obtained as the output of the first step of the procedure. Thus, by introducing the MTRFs in the first step of the procedure, the problem of matching the seismograms is transformed to the problem of matching the MTRFs. The advantage is evident: there are always six MTRFs at most, and their sampling can be modified with respect to the sampling of the observed seismograms, which allows us to reduce the system of equations for the searched source parameters.

This is not, however, the principal advantage of the two-step algorithm. Its major benefit is the capacity of the MTRFs, which are 'overparametrized' in the first step, being considered as independent functions, to capture spurious signals originating from the deconvolution of an inexact GF from the observed records. These spurious signals are assumed to be expressed in the deconvolved MTRFs in two ways. First, we deal with weak events only (throughout we make the point-source approximation), where we feel it is reasonable not to expect a change in the mechanism during rupture. Thus, if we knew the medium exactly, that is if our GFs were correct, the deconvolved MTRFs would be linearly dependent, $\dot{M}_{ij}(t) \rightarrow M_{ij}\dot{M}(t)$. The departures from linear dependence we attribute to a violation of this assumption, and, thus, we search for the correlated part of the MTRFs only. Second, we choose to assume that there is no obvious physical reason for the occurrence of a reverse slip during rupture in the foci of weak events. If a reverse slip occurs in the deconvolved MTRFs, we attribute it to an inconsistency between the GFs and the data;

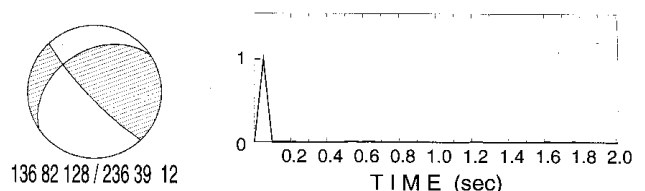


Figure 1. Source model used for the generation of synthetic data: the mechanism is a combination of dip-slip with a minor strike-slip component (left); STF δ -pulse (right). The fault-plane solution represents the mechanism determined from *P*-wave polarities for the February 1988 Friuli event studied in the final section of this paper. Strike, dip, and rake of nodal planes are given below the lower hemisphere projection.

that is to an effect of a poor modelling of the structure. If reverse slip is felt credible, though, it will be contained in the first part of the inversion, and so will be accessible. Therefore, we search for the positive STF; that is, only one side of the MTRFs is kept. The ambiguity of deciding about the sign is avoided by seeking for a mechanism that is consistent with the available clear readings of first-arrival polarities.

We compare the ability of Method I to suppress the spurious effects of poor structure modelling with the performance of

an approach imposing *a priori* constraints on the source, Method II (Mao, Panza & Suhadolc 1994). Method II assumes *a priori* a double couple and a positive STF, parametrized by a sequence of delayed overlapping triangles. The depth of the hypocentre is optimized simultaneously with strike, dip and rake angles of the double couple and weights of the triangles describing the STF. A gradient scheme is applied and the algorithm proceeds iteratively from a starting point which must be sufficiently close to the solution of the problem.

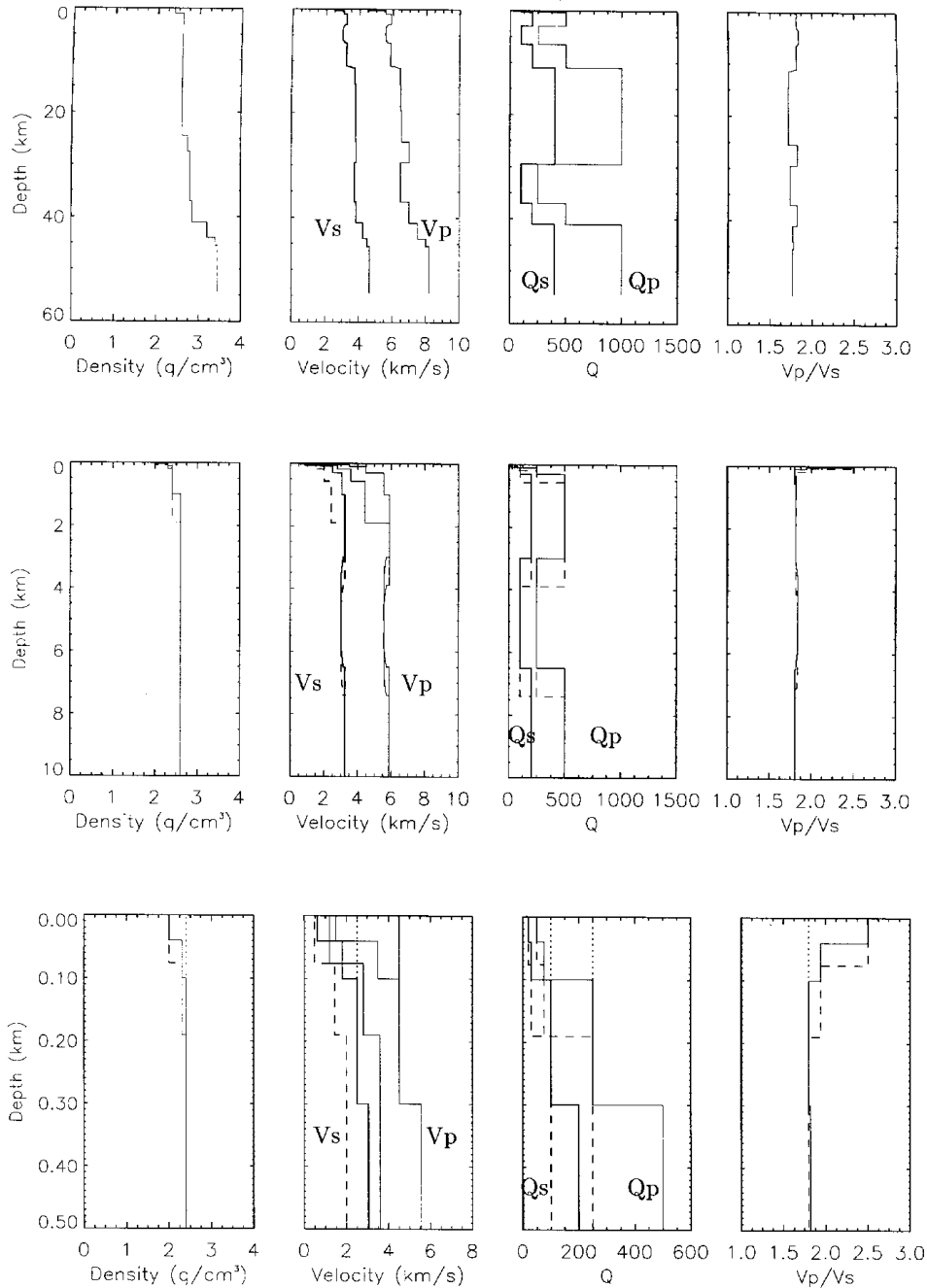


Figure 2. Structural models of the Friuli area, northeastern Italy. FRIUL7W: standard model (solid line) used to construct the GF; FRIUL7M: modified standard model eliminating the near-surface low-velocity layers at the top of the structure (dashed line); FRIUL7P: modified standard model with a thicker low-velocity zone (dotted line). Top row: standard model to a depth of 60 km; middle row: FRIUL7W and FRIUL7P to a depth of 10 km; bottom row: the upper 0.5 km for the three models.

COMPARISON OF THE TWO APPROACHES USING SYNTHETIC DATA

To demonstrate the ability of Method I to yield a reasonable STF even with an inadequate GF, and to check that Method II does not, the following synthetic experiment is performed. For the configuration of the local seismic network operating in Friuli, NE Italy, synthetic high-frequency vertical-component seismograms are generated for the model of a double-couple point source with both strike-slip and dip-slip components, characterized by an instantaneous moment release—see Fig. 1. In practice, the structure of the propagation path will vary between stations: for the Friuli Network, there are stations situated on the plain where there is a thick cover of sediments characterized by low velocities, and some stations operate in the mountains where slow sediments are largely absent—see Fig. 2. Therefore, two synthetic experiments are implemented: one with large velocity contrasts between stations and one with smaller contrasts. In the experiment with lower heterogeneity, the synthetic seismograms—‘observed’ data for the inversion—are computed using the standard 1-D model for the region, FRIUL7W (see Fig. 2 of Mao & Suhadolc 1992), for stations UDI, RCL, CAE. The remaining stations—those situated in the mountain zone of the region—are assigned to a modified structural model FRIUL7M, differing from the standard model FRIUL7W in the top 0.2 km where the velocities are higher (see Fig. 2). In the experiment with greater heterogeneity, the stations of the mountain zone keep the seismograms synthesized with the model FRIUL7M, while for

the remaining stations (UDI, RCL, CAE), the data are computed with the model FRIUL7P, which simulates the thick sedimentary cover in this zone of the Friuli region (see Fig. 2). The modified models FRIUL7M and FRIUL7P are designed only with the aim of testing the performance of waveform-inversion algorithms in the presence of an inconsistency in the modelling of the structure, and, thus, we do not claim that they are totally appropriate from a geological viewpoint. What is important in the experiments is that the ‘observed’ data are all inverted using a GF constructed with the standard model FRIUL7W. This means inconsistency is introduced in the forward modelling: in the low-level heterogeneity experiment the GF is consistent with the records of stations UDI, RCL, CAE, while in the high-level heterogeneity test it is consistent with none of the seismograms.

Because the models FRIUL7P and FRIUL7M differ from FRIUL7W in the upper layers only, we can expect the introduced inconsistency to have a different influence in the search for parameters of a shallow and of a deep source. Therefore, for each experiment, two source depths are considered: 4.37 km and 8 km. The location of the epicentre is favourable for the determination of the mechanism, since it is situated within the network (see Fig. 3).

For each experiment data are generated with low-frequency (LF) content (up to 3 Hz), and with high-frequency (HF) content (up to 10 Hz). As expected, the inversion of the LF data yields a mechanism and a STF closer to the true source parameters than the inversion of the HF data because, at low frequencies, the inconsistency of the forward modelling is less

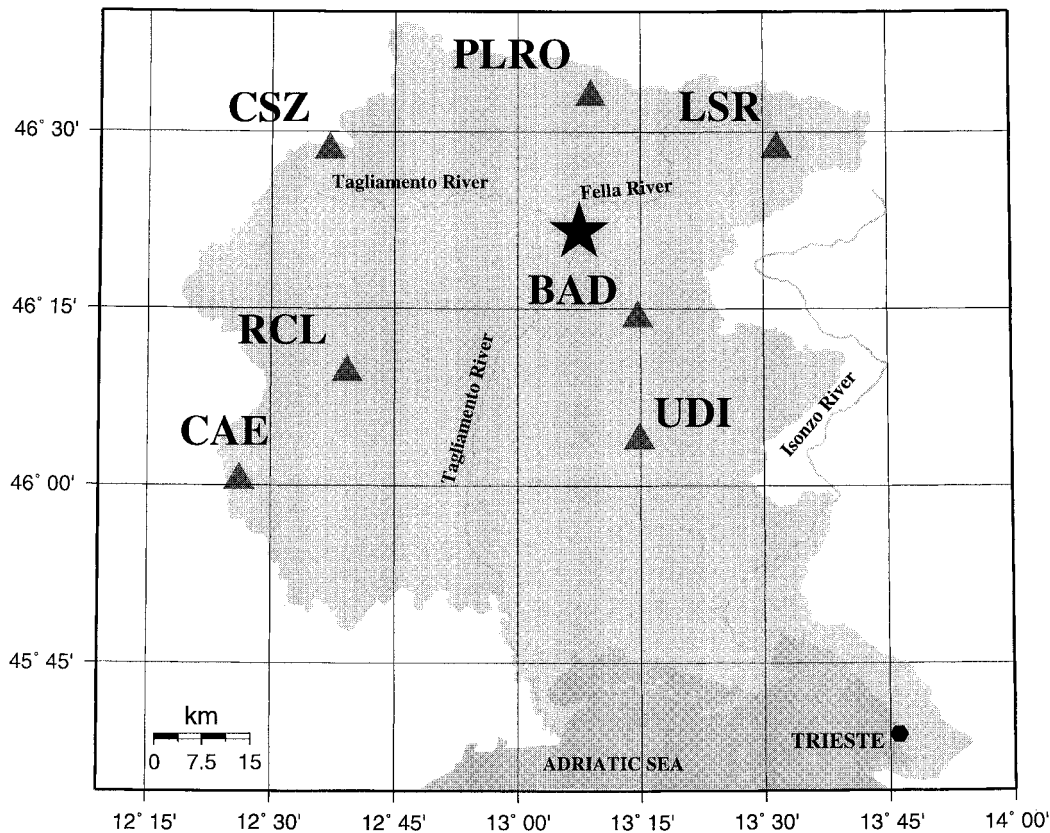


Figure 3. Friuli region, northeastern Italy. Triangles: seismic stations; star: epicentre. Axes are latitude and longitude in degrees.

significant than at high frequencies: the latter 'see' finer details of the structure. Our aim is to explore the behaviour of the inverse algorithms discussed in extreme conditions; thus, in the following only the HF experiments are presented.

An important technical parameter heavily influencing the performance of the inverse algorithms is the damping of the solution of the normal equations (Koch 1991a), which stabilizes the solution if the equations are poorly conditioned. On the

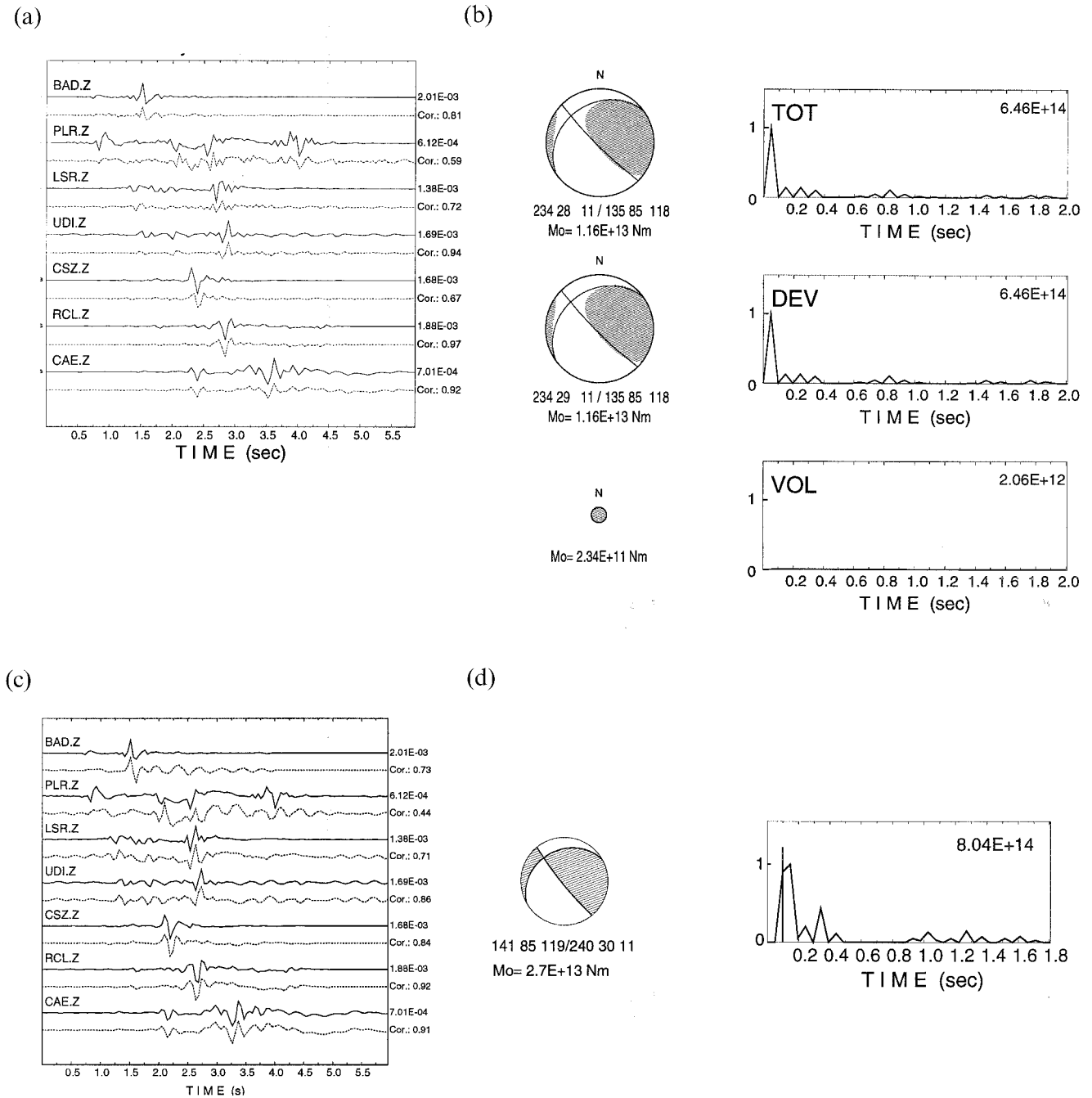


Figure 4. Synthetic experiments with a slight inconsistency of the GF (shallow event). The vertical segment marks the origin time (T_0) of the synthetic signals. Here and in all following figures, dip, slip and rake of the nodal planes and the scalar seismic moment (M_0) are given below the plot of the mechanism (lower-hemisphere projection). The value inside the STF plot is the ratio between the scalar seismic moment (M_0) and the area of STF. *Method I* (a) Data (solid lines) and modelled vertical-component seismograms (dashed lines); the values at the right-hand side are respectively maximum amplitude and correlation between observed and synthetic data for each station. (b) Source mechanism and STF obtained with the factorization of the complete MTRFs (TOT), of the deviatoric (DEV) and the volumetric (V) components. Hatched areas: compressions; solid lines: nodal planes of the corresponding best double couple. Here and in the following figures the diameter of the projection sphere is proportional to the scalar moment of each source component. *Method II* (c) Data (solid lines) and modelled seismograms (shaded line); the values at the right-hand side are respectively maximum amplitude and correlation between observed and synthetic data for each station. (d) Mechanism and STF.

other hand, it limits the resolution of the model parameters that are sought. Empirically, we find that a damping reaching about 0.01 of the maximum on the diagonal of the normal equation matrix represents a good compromise.

Small inconsistency

The records in four stations (BAD, PLR, LSR and CSZ) out of the seven correspond to the model FRIULM; that is, they are inconsistent with the GF (constructed for FRIUL7W). Both models differ in the upper layers only, and thus a limited effect should be expected. In fact, the seismograms in the two-step inverse scheme applied to the shallow event are modelled very well both for stations with consistent and inconsistent data, except for the beginning of the record at PLR—see Fig. 4(a). The source parameters recovered are very close to the true ones (both mechanism and STF)—see Fig. 4(b): there is only very little spurious volumetric (V) component (see Table 1), and the deviatoric part of the tensor contains a small portion of compensated linear vector dipole (CLVD), the orientation of which is nearly the same as that of the true source. The reconstruction of the STF is even more satisfying: there is a very well pronounced single peak at the very beginning, followed by a tail of negligible amplitude. On the other hand, Method II yields a far less satisfying STF, in which the spurious tail following the highest peak at the beginning is very strong and reaches about half of the amplitude of the principal peak (Fig. 4c). Moreover, the principal peak in the resolved STF extends for two sampling steps, while the true STF is a δ -function; that is, even if we neglect its tail the duration of the STF remains overestimated. The mechanism obtained with Method II is nearly the true one; however, this success is rather fictitious since the solution is *a priori* constrained to be a double couple and the inverse scheme applied is a gradient method proceeding in iterative steps and, thus, needs a good starting point, which we choose to be the true mechanism. When beginning from another mechanism, the procedure may fail to converge, while Method I is completely independent of a starting point both for the mechanism and the STF.

Since the FRIUL7M and FRIUL7W models differ in the top layers only, the inconsistency should be less important when the records generated by a deeper source are inverted. This is confirmed by the results of the two-step algorithm: the

spurious V component is decreased in comparison with that retrieved for the shallow focus, compare Figs 4(b) and 5(a), and the orientation of the deviatoric part and the STF are well determined. On the other hand, the STF obtained by

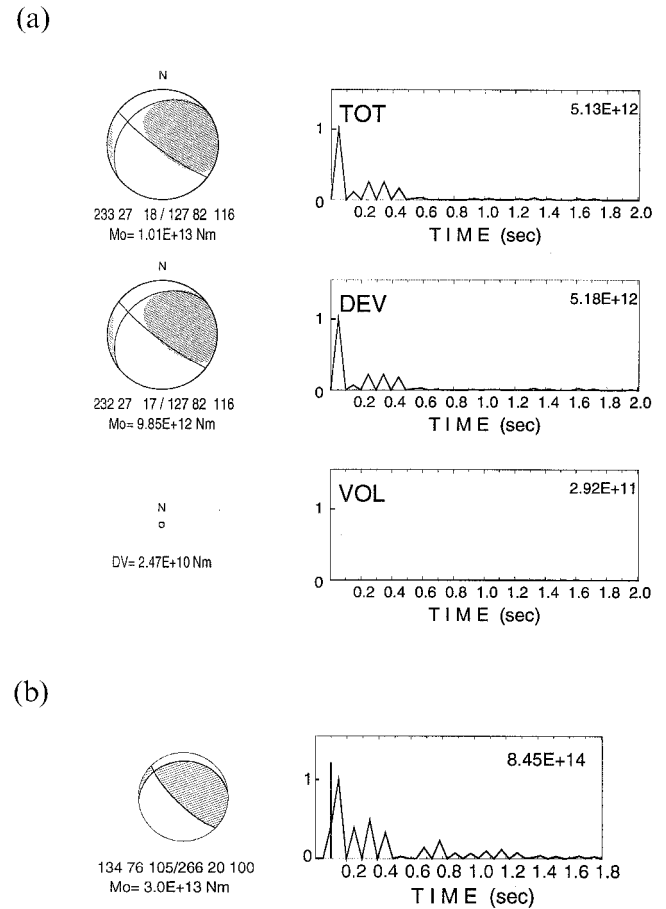


Figure 5. Synthetic experiment with a strong inconsistency of the GF (deep event). (a) Method I: mechanism and STF obtained by the factorization of the complete MTRFs (TOT), of the deviatoric (DEV) and the volumetric (V) components. Hatched areas: compression of the moment tensor solution; solid lines: nodal planes of the corresponding best double couple. (b) Method II: the resolved mechanism and STF.

Table 1. Comparison of the results obtained using synthetic data. Method I—two-step algorithm: (1) linear inversion of seismograms; (2) factorization of independent MTRFs into STF and moment tensor; Method II—*a priori* constrained to a non-negative STF and to a DC mechanism. The GFs have been computed for the model FRIUL7W. Results of synthetic experiments with data up to 10 Hz. Low inconsistency: synthetic data generated using models FRIUL7W and FRIUL7M; high inconsistency: synthetic data generated using models FRIUL7M and FRIUL7P. S: shallow focus; D: deep focus. Δ : difference between resolved and true depth, strike, dip, and rake angles, respectively. Mo_{TOT}/Mo_{True} and Mo_{DEV}/Mo_{True} : ratios of resolved TOT and DEV scalar moment, respectively, to the scalar moment of the true source. Mo_{VOL}/Mo_{DEV} ratio of the VOL and DEV components of the resolved moment tensor. STF length estimate of the length of the resolved STF; Tail/Peak Ratio: rough estimate of the ratio between the amplitude of the principal peak in the resolved STF to the amplitude of the remaining part.

| Event | METHOD I | | | | | METHOD II | | | | | | | | |
|--------|---------------------|------------------------|---------------------|----------------------|------------------|------------------|------------------|-----------------|------------------|---------------------|-------------|-----------------|------------------|------|
| | Δ Depth (km) | Δ Strike (deg.) | Δ Dip (deg.) | Δ Rake (deg.) | Mo Tot./ Mo True | Mo Dev./ Mo True | Mo Vol./ Mo Dev. | STF Len. (sec.) | Tail/ Peak Ratio | Δ Depth (km) | Mo/ Mo True | STF Len. (sec.) | Tail/ Peak Ratio | |
| Low | S | 0.00 | -1 | +3 | -10 | 1.13 | 1.13 | 0.020 | 0.77 | 0.13 | -0.03 | 2.7 | 1.30 | 0.89 |
| Incon. | D | 0.00 | -9 | 0 | -12 | 0.99 | 0.97 | 0.002 | 0.41 | 0.25 | -0.01 | 3.0 | 1.30 | 0.68 |
| High | S | +0.20 | +32 | 0 | +11 | 1.40 | 1.39 | 0.025 | 0.82 | 0.32 | -0.01 | 5.5 | 1.70 | 0.99 |
| Incon. | D | -0.10 | -2 | 0 | -33 | 1.54 | 1.67 | 0.025 | 0.86 | 0.54 | -0.03 | 12.0 | 1.55 | 0.68 |

Method II remains poorly resolved: the width of the principal peak is doubled with respect to the true STF, and the spurious amplitudes in the tail reach about half of the amplitude of the initial peak (Fig. 5b).

Large inconsistency

Similarly to the previous experiment, in the stations situated in the mountain zone of the area (i.e. BAD, PLR, LSR and CSZ) the data are generated using the model FRIUL7M (Fig. 1). However, for stations on the plain (UDI, RCL, and CAE) the data are generated using the FRIUL7P model, representing quite a large departure from the standard structure

FRIUL7W. Thus no station has an appropriate seismogram for the model used in inversion.

The very large inconsistency of the forward modelling, due to the introduction of the model FRIUL7P, represents a very severe test of the capability of the inverse methods to deal with inappropriate structural models. A strong inconsistency of the ‘observed’ records with the GF is inherent in all the synthetics based on the FRIUL7P structure, especially UDI and CAE which do not model the ‘records’ very successfully (Fig. 6a). Despite that, the source parameters yielded by Method I are fairly satisfactory with respect to the result of the previous test with the ‘low inconsistency’: the mechanism is slightly rotated (especially the strike angle), and the V

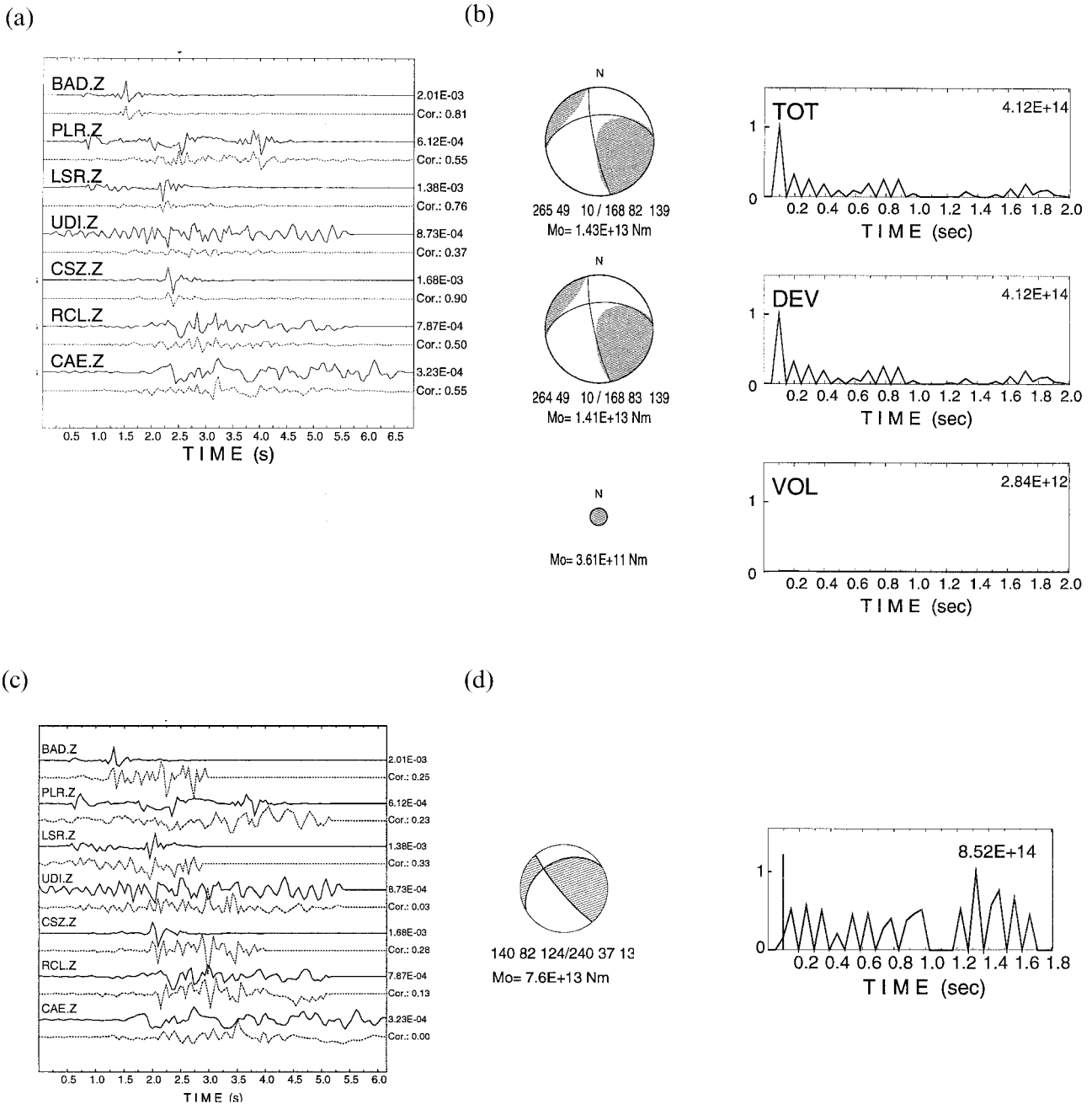


Figure 6. Synthetic experiment with a strong inconsistency of the GF (shallow event). For details see the caption of Fig. 4.

component is a little larger (Fig. 6b). The amplitude of the spurious tail of the STF in Fig. 6(b) is larger than in Fig. 4(b), but the narrow peak occurring at its beginning can be clearly identified. The shift in the arrival time is due to the depth of the relocated hypocentre, which is different from the depth of the true focus—see Table 1. On the other hand, Method II appears to be much less successful. The resolved STF is quite different from the true one both in shape and duration: the group that could be marked as the major one consists of few peaks of comparable amplitudes, and if we approximate it by a smooth envelope its duration is very long with respect to the δ -pulse of the true STF—see Fig. 6(c).

Returning to Method I, the deep event is strongly affected by the inconsistency of the forward modelling. The spurious V component is smaller than in the case of the shallow source, but the orientation of the deviatoric part departs more from the true mechanism. One of the nodal planes is modelled very well, but the other one is inclined substantially, annihilating the strike-slip component of the source (compare Figs 7(a) and 1); the resolved STF are rather complex, but at least after the factorization of the complete MTRFs we obtain a STF where a dominant peak can be recognized. However, its width is doubled with respect to the true STF and the tail is of rather high amplitude, which results in the overestimation of the rupture duration. As could be expected, Method II provides even less reliable information on the source process: the resolved STF is entirely distorted (Fig. 7b).

Using a variant, more suitable for our case, of the Rogers & Pearce (1987) representation, in Fig. 8 we summarize the

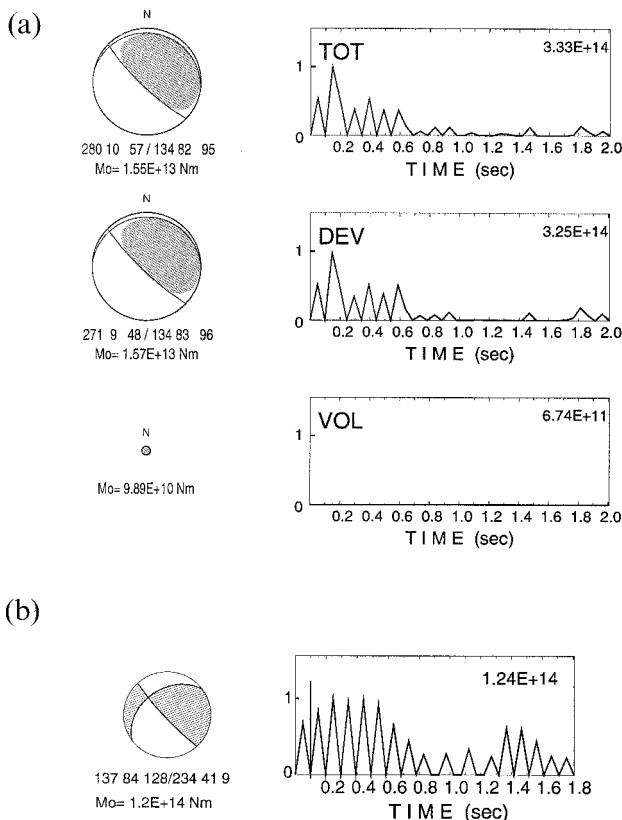


Figure 7. Synthetic experiment with a strong inconsistency of the GF (deep event). For details see the caption of Fig. 5.

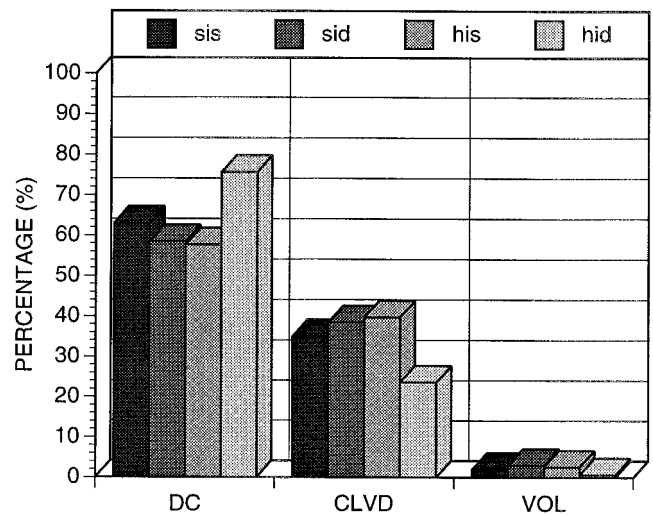


Figure 8. Histograms summarizing the results of the synthetic tests made with Method I. Percentages of DC, CLVD and V. sis: small inconsistency, shallow source; sid: small inconsistency, deep source; his: high inconsistency, shallow source; hid: high inconsistency, deep source.

overall results of the tests for Method I. The dominant part of the source is still double couple, but there is a large CLVD component whose percentage does not seem to be related to the inconsistency of the structural model or to the source depth location. Obviously, when LF data are used, the two methods retrieve results that are more stable and closer to the original source parameters: even if Method I remains superior to Method II, the performances of the two methods get closer.

FRIULI EVENT

We illustrate the application of the two methods to an $M_d = 3.0$ event belonging to the swarm that occurred in 1988 February close to Moggio Udinese in the Friuli area (NE Italy).

The short-period records of the North-Eastern Italy Seismometric Network (Fig. 3) were low pass filtered at 3 Hz (because, according to synthetic experiments, LF data appear less sensitive, but not insensitive, to the inconsistency of the structural model than HF data), and the instrumental responses were convolved with synthetic signals. With Method I all the GFs are computed for the FRIUL7W structural model using the same vertical grid for the hypocentral depth as used in the synthetic experiments. From Fig. 9(a) one can see a good correlation between the observed and the synthetic signals, and only UDI, CSZ and CAE are partially modelled. The orientation of the nodal planes is fairly close to the one retrieved from the first-motion polarity analysis (Fig. 1). The STF has two small peaks after 0.3 s, and two larger ones from 1 s onwards; the volumetric component is negligible as expected for a tectonic event (Fig. 9b). The retrieved hypocentral depth, $h = 4.2$ km, is 5 per cent smaller than the one obtained from P traveltimes analysis. If we take into account the noise level present in the signals, the first part of the STF is not completely resolved (Fig. 9c) but the retrieved hypocentral depth is $h = 4.2$ km.

When using Method II, if we start from the source model and hypocentral depth given by first-arrival analysis there

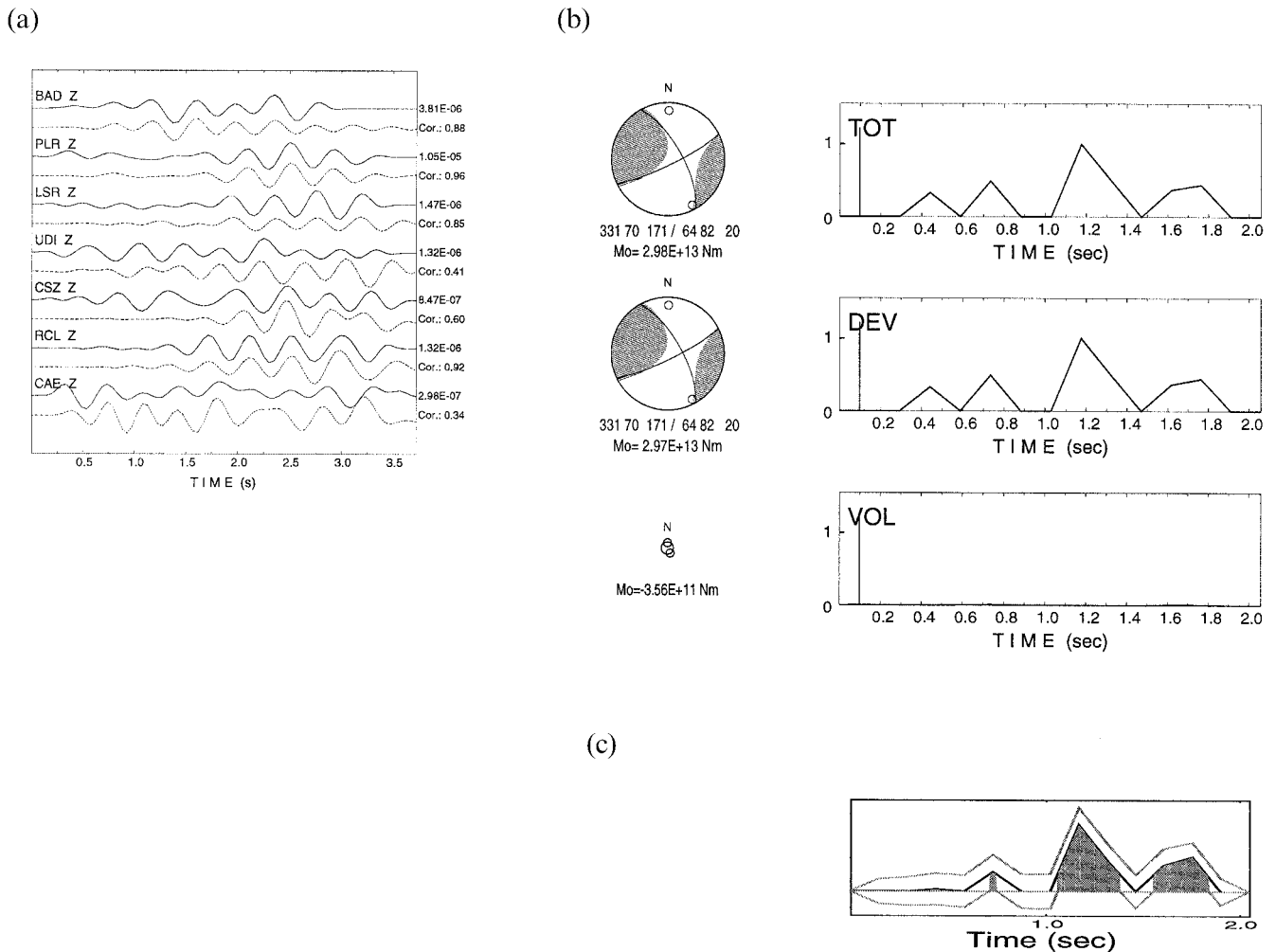


Figure 9. Event of 1988 February 2, at 10h23m UTC, processed with Method I. (a) Observed (solid) and synthetic (dashed) signals. (b) Retrieved mechanism and STF for TOT, DEV, and V components. The two small open circles on the focal sphere projection correspond to clearly readable (negative) first arrivals. The vertical segment marks T_0 , computed from P -wave arrivals. (c) Noise effect on STF; the dark areas show the reliable parts of the STF taking into account the error bars (Cespuglio, Campus & Sileny 1996).

is no convergence, while the convergence is assured starting from the source model and hypocentral depth retrieved with Method I (Fig. 10). With Method II the retrieved hypocentral depth is $h = 4.0$ km.

CONCLUSIONS

To retrieve the source parameters from waveform inversion it is necessary to model the medium as well as possible. However, exact knowledge of the medium is the exception rather than the rule: in practice, we have only rough estimates of the structure. Structural complexities which are not included in the model of the medium, that is which are not modelled in the GF, are projected, after deconvolving the GF from the seismograms, into the source parameters, especially the STF, where they appear as spurious signals distorting its true shape.

This unwelcome effect depends on the parametrization of the source. If we avoid constraining the source model *a priori* to a non-negative STF and a constant mechanism, we suppress the artefacts of poor structure modelling. The two-step algorithm consisting of (1) parametrizing the source by independent

MTRFs and (2) their subsequent reduction into the non-negative STF proved to have a capacity to absorb the spurious effects of inexact modelling of the structure in the ‘over-parametrized’ MTRFs and to minimize these effects during the search for the constrained STF. This approach, implying an *a posteriori* constraint, is demonstrated to be more successful in inverting seismic records by means of an inconsistent structural model than a traditional method implementing *a priori* constraints. In particular, it provides us with a better estimate of the STF: overestimation of its duration yielded by the *a priori* constrained method is largely avoided here.

The dominance of the two-step algorithm over the gradient method employing the *a priori* constrained parametrization is demonstrated by processing the records of the Friuli event: the latter method does not converge unless it knows the solution of the former as the starting point.

ACKNOWLEDGMENTS

We acknowledge financial support from Grant A3012601 of the Grant Agency, Acad. Sci. Czech Rep., Copernicus CIPA

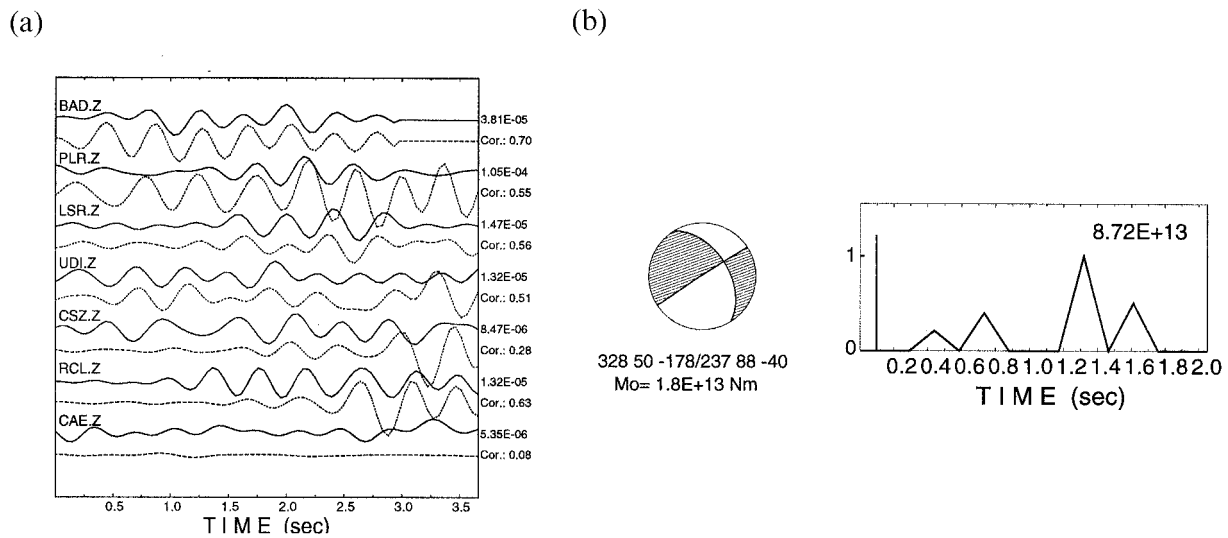


Figure 10. Event of 1988 February 2, at 10h23m UTC, processed with Method II starting from the mechanism and source depth obtained with Method I. (a) Observed seismograms. (b) Retrieved mechanism and STF. The vertical segment marks T_0 .

CT 94-0238, INCO-Copernicus IC15 CT96200, Programma Nazionale di Ricerche in Antartide (PNRA), Progetto 1b-c; Struttura ed evoluzione dei Bacini Periantartici e dei Margini della Placca Antartica, MURST 40 per cent and 60 per cent funds, and CNR contract number (96.00318.05), and Foreign Affairs of the Italian Government in the frame of Law 212.

REFERENCES

- Cespuglio, G., Campus, P. & Sileny, J., 1996. Seismic moment tensor resolution by waveform inversion of a few local noisy records—II. Application to the Phlegraean Fields (Southern Italy) volcanic tremors, *Geophys. J. Int.*, **126**, 620–634.
- Dahm, T., 1996. Relative moment tensor inversion based on ray theory: theory and synthetic tests, *Geophys. J. Int.*, **124**, 245–257.
- Hartzell, S.H., 1978. Earthquake aftershocks as Green's functions, *Geophys. Res. Lett.*, **5**, 1–4.
- Koch, K., 1991a. Moment tensor inversion of local earthquake data—I. Investigation of the method and its numerical stability with model calculations, *Geophys. J. Int.*, **106**, 305–319.
- Koch, K., 1991b. Moment tensor inversion of local earthquake data—II. Application to aftershocks of the May 1980 Mammoth Lakes earthquakes, *Geophys. J. Int.*, **106**, 321–332.
- Langston, C.A., Barker, J.S. & Pavlin, G.B., 1982. Point-source inversion techniques, *Phys. Earth planet. Inter.*, **30**, 228–241.
- Mao, W.J. & Suhadolc, P., 1992. Simultaneous inversion of velocity structures and hypocentral locations: application to the Friuli seismic area NE Italy, *Pageoph.*, **138**, 267–285.
- Mao, W.J., Panza, G.F. & Suhadolc, P., 1994. Linearized waveform inversion of local and near-regional events for source mechanism and rupture processes, *Geophys. J. Int.*, **116**, 784–798.
- Nabelek, J.L., 1984. Determination of earthquake source parameters from inversion of body waves, *PhD thesis*, MIT, Cambridge University, MA.
- Rogers, R.M. & Pearce, R.G., 1987. Application of the relative amplitude moment-tensor program to the three intermediate-depth IASPEI earthquakes, *Phys. Earth planet. Inter.*, **30**, 93–106.
- Ru, L.J. & Tichelaar, B.W., 1990. Moment tensor rate functions for the 1989 Loma Prieta earthquake, *Geophys. Res. Lett.*, **17**, 1187–1190.
- Sileny, J., Panza, G.F. & Campus, P., 1992. Waveform inversion for point source moment tensor retrieval with variable hypocentral depth and structural model, *Geophys. J. Int.*, **109**, 259–274.
- Sileny, J. & Psencik, I., 1995. Mechanisms of local earthquakes in 3-D inhomogeneous media determined by waveform inversion, *Geophys. J. Int.*, **121**, 459–474.
- Sileny, J., Campus, P. & Panza, G.F., 1996. Seismic moment tensor resolution by waveform inversion of a few local noisy records—I. Synthetic tests, *Geophys. J. Int.*, **126**, 605–619.
- Sipkin, S.A., 1982. Estimation of earthquake source parameters by the inversion of waveform data: synthetic waveforms, *Phys. Earth planet. Inter.*, **30**, 242–259.
- Stump, B.V. & Johnson, L.R., 1977. The determination of source properties by the linear inversion of seismograms, *Bull. seism. Soc. Am.*, **67**, 1489–1502.
- Vasco, D.W., 1989. Deriving source-time functions using principal component analysis, *Bull. seism. Soc. Am.*, **79**, 711–730.